

## Novel Axisymmetric Coherent Vortex State in Arrays of Josephson Junctions Far from Equilibrium

D. Domínguez,<sup>(a)</sup> Jorge V. José, and Alain Karma

*Physics Department, Northeastern University, Boston, Massachusetts 02115*

C. Wiecko

*Centro Atómico Bariloche, 8400 San Carlos de Bariloche, Rio Negro, Argentina*

(Received 9 July 1991)

We present a numerical study of a topologically disordered, overdamped, array of Josephson junctions subjected to dc and ac currents. We find that vortices are nucleated by the ac current, apart from the ones produced at defects. After a complex transient, these vortices settle into a parity-broken time-periodic, *axisymmetric coherent vortex state* characterized by rows of vortices lying along a tilted axis. This locked-in state leads to giant *half-integer* pseudosteps in the  $I$ - $V$  characteristics that are hysteretic in nature. Possible connections of these results to recent experiments are discussed.

PACS numbers: 74.50.+r, 74.60.Jg, 85.25.Dq

Arrays of Josephson junctions (AJJ) have been the subject of considerable recent interest, both theoretically and experimentally [1]. Many of the early studies in AJJ were aimed at testing the predictions of the equilibrium long-range phase-coherent transitions expected to take place in these systems [2]. More recently, novel phenomena have been discovered in the dynamic responses of the arrays subject to time-dependent periodic probes. Giant Shapiro steps (GSS) in the  $I$ - $V$  characteristics of *periodic* proximity-effect AJJ have been measured in zero [3] and rational frustration magnetic fields [4]. These results have led to a series of numerical and analytic analyses that have for the most part been successful in explaining the GSS results [5,6]. One exception is the recent report of half-integer pseudosteps seen in Nb-Au-Nb AJJ [7]. In this paper we present results that yield half-integer pseudosteps that may be related to these experiments.

Here we study the dynamics of defect and current-nucleated vortices as a result of a current  $I_a = I_{dc} + I_{ac} \times \sin(2\pi\nu t)$ , applied uniformly from the bottom of the AJJ along the  $y$  direction. The formation of vortex pairs by defects in a dc current at zero temperature was studied recently by Leath and Xia [8]. These authors emphasize the formation of these excitations as an example of breakdown phenomena. The new element in our investigation is that of adding an ac current to the study of the dynamics of the defect-generated vortices in AJJ. It turns out that adding an ac current changes the physics in a fundamental way as we shall discuss below. We have studied the dynamics of the AJJ when we have one, two, three, or all the lattice sites randomly displaced from their periodic positions. We have found that after a transient time that depends on the number of defects, the dynamics tends to a nonequilibrium time-periodic state with a well-defined vortex geometric structure that is qualitatively and to some extent quantitatively independent of the nature and number of defects in the system. This novel state leads to half-integer giant pseudosteps in the  $I$ - $V$  characteristic. This state is in many respects different in nature from the GSS mentioned above and

we shall call it an *axisymmetric coherent vortex state* (ACVS). Since the existence of the ACVS does not appear to depend qualitatively on the number of defects in the lattice, most of our discussion here will be related to the one-defect problem, but we present some results for the all-site-disordered case as well. A more extensive and detailed discussion of all the cases studied will appear elsewhere [9].

The model is defined by an  $L_x L_y$  AJJ, where the location of each superconductor forming the junctions is given by a two-dimensional vector  $i$ . The present study is based on the resistively shunted junction model that has been successful in explaining the GSS. The equations of motion are given by

$$\Gamma_{ij} \frac{\partial \phi_{ij}}{\partial t} = \frac{\delta S}{\delta \phi_{ij}} + \eta_{ij}, \quad (1a)$$

where the action  $S$  is defined as

$$S = \sum_{ij} \frac{\hbar}{2e} [I_{ij} \cos(\phi_{ij} + 2\pi f_{ij}) + \phi_{ij} I_{ij}]. \quad (1b)$$

In Eqs. (1),  $\phi_{ij} = \phi_i - \phi_j$  is the phase difference between the superconductors  $i$  and  $j$  making the junction,  $I_{ij}$  is the total current flowing between them,  $I_{ij}^c$  is their critical current, and  $\Gamma_{ij} = \hbar/2eR_{ij}$  with  $R_{ij}$  their normal-state resistance. The Gaussian random variable  $\eta_{ij}$  represents thermal fluctuations with covariance

$$[\eta_{il}(t)\eta_{kj}(t')] = \delta_{il,kj} \delta(t-t') \hbar^2 k_B T / 4e^2 R_{kl}.$$

The effect of a transverse magnetic field is given by the line integral  $f_{ij} = (1/\Phi_0) \int_i^j \mathbf{A} \cdot d\mathbf{l}$ , with  $\mathbf{A}$  the magnetic vector potential, and  $\Phi_0$  the flux quantum. Current conservation is given by Kirchoff's conditions at each lattice site,  $\sum_j I_{ij} = I_i^{\text{ext}}$ , with  $I_i^{\text{ext}}$  the external current at site  $i$ . The effect of the applied current  $I_a$  enters as boundary conditions at the bottom of the array while the voltages at the top of the array are set to zero. Most of our calculations utilize periodic boundary conditions, but we have also compared our results when we use free boundary conditions. We have found, however, that since the lat-

tices we are able to simulate are relatively large, there are no qualitative differences between the two types of boundary conditions. We approximate  $R_{ij}=R$  and  $I_{ij}^f=I_c$ . All equations are rewritten in dimensionless units with time normalized by the natural frequency  $\nu_0=2eRI_c/\hbar$ , the currents by  $I_c$  (and denoted by  $i_{dc}$  and  $i_{ac}$ ), and temperature by  $\hbar I_c/2k_B e$ . The time-averaged voltage  $\langle V \rangle$  is normalized by  $(\hbar\nu/2e)L_y$ , so as to assume integer values at the zero-field GSS.

It turns out that being able to simulate large lattices is important for finding the ACVS. We solved the equations of motion given in Eqs. (1) by using a variation on the pseudospectral method [10]. Our method consists of calculating the fast Fourier transform (FFT) of the equations of motion along the  $x$  direction, solving the tridiagonal equation for  $\phi$  along the  $y$  direction, and then carrying out the time integration using a fourth- or second-order Runge-Kutta (RK) method. Eikmans and van Himbergen [6] have applied a similar method by doing the FFT along the  $x$  and  $y$  directions. Our method shows an improvement of about 30% over theirs. We have also done calculations at finite temperature, extending the second-order RK algorithm developed by Greenside and Helfand [11]. The time steps taken in our calculations ranged from  $\nu_0\Delta t=0.1$  to 0.01 and typical runs used ranged from one to several thousand time steps.

We now discuss our results starting with the one-defect case. We produce the defect by moving a lattice site radially away from its periodic position. This only changes the  $f_{ij}$  in Eq. (1). By taking integer  $f$ 's, with  $f$  defined as  $f=\Phi/\Phi_0$ , where  $\Phi=\sum_{\mathcal{P}(R)}f_{ij}$ , and  $\mathcal{P}(R)$  denotes the plaquette located at  $R$ , this change is only felt along the bonds linked to the defect. Thus when we talk about having or not having a defect we mean having  $f$  an integer or equal to zero, respectively. We take the defect to be either at the center of the lattice or off center. It turns out that the location of the defect site does not affect the formation of the ACVS. In Fig. 1 we show the corresponding results for the  $I$ - $V$  characteristics for different cases. Figure 1(a) shows the GSS for the periodic case for comparison. In Fig. 1(b), for the one-defect case, we clearly see new pseudo half-integer steps (PHIS) at voltage values  $\langle V \rangle = \frac{1}{2}$  and  $\frac{3}{2}$ . We see the PHIS for higher currents although less clearly. A blowup of Fig. 1(b) is shown in Fig. 1(d), showing the hysteretic behavior for increasing and decreasing dc current. This hysteretic behavior is not seen in the GSS. We call them pseudosteps because their slope is not exactly zero as in the GSS. The oscillations below the  $\langle V \rangle = \frac{1}{2}$  PHIS are characteristic of the specific location of the defect. These oscillations get smoothed out when increasing the number of defects as seen in the glass case shown in Fig. 1(e). We carried out a size analysis of the width at the  $n = \frac{1}{2}$  PHIS and found that there is a minimum critical size above which it becomes visible. These results are shown in Fig. 2(a). Here the need to have an efficient algorithm allowing large lat-

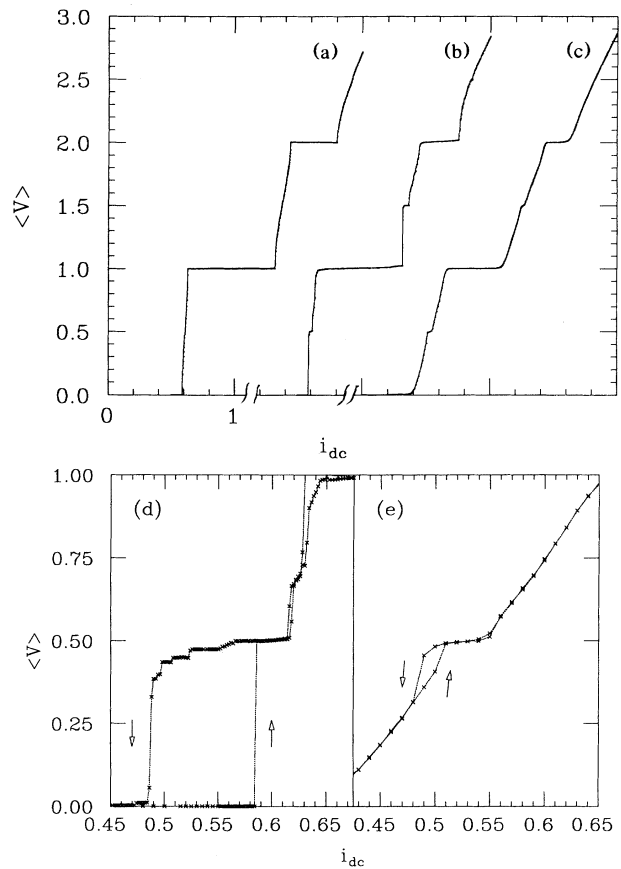


FIG. 1. Zero-temperature  $I$ - $V$  characteristics for square arrays of size  $40 \times 40$ , with  $i_{ac}=1$ ,  $\nu=0.1\nu_0$ , and periodic boundary conditions. (a) Periodic case ( $f=0$ ). (b) One defect in the center with  $r=0.1$ ,  $\theta=90^\circ$ , and  $f=2$ . (c) Glass case with  $\epsilon=0.1$ . The results correspond to quenched averages over five samples. For clarity the curves in (b) and (c) are shifted by one and two units, respectively. (d) Blowup of (b) showing the hysteretic behavior. (e) The same as (d) for (c).

tice simulations becomes evident. We calculated the spectral function,

$$S(\nu) = \lim_{\tau \rightarrow \infty} \left| \frac{1}{\tau} \int_0^\tau V(t) e^{i2\pi\nu t} dt \right|^2,$$

and found that the ACVS has resonances at frequencies  $\nu$  and  $\nu/2$ , confirming the characteristic of the PHIS. It was at this point that we were rather intrigued by these results and so we decided to explicitly visualize what the vortices were doing; we made a series of movies describing their dynamical evolution. The movies show the following facts: When increasing  $i_{dc}$ , with  $i_{dc} < i_c^+ = 0.584$ , the current has the effect of nucleating a vortex pair, as seen by Leath and Xia, but in this case the vortex dipole oscillates in polarity in tune with the ac current. This state is stable for the longest times considered. Exactly

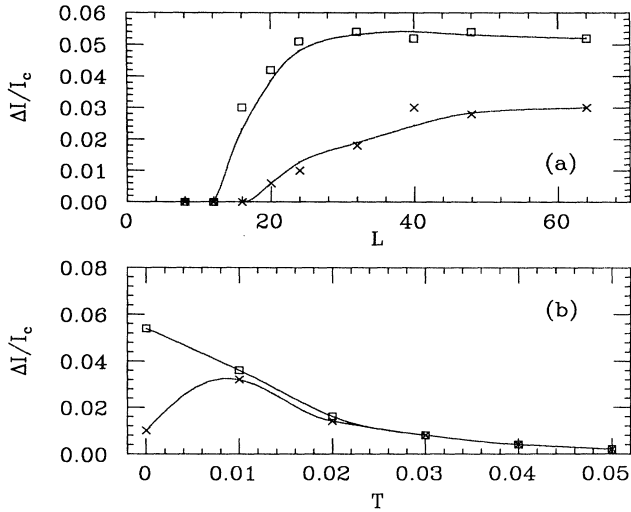


FIG. 2. Step width for one defect when  $\langle V \rangle = \frac{1}{2}$ . (a) As a function of the size of a lattice  $L \times L$ . (b) As a function of temperature  $T$  ( $L = 40$ ). Increasing ( $\square$ ) and decreasing ( $\times$ ) the current.

the same situation occurs when sitting at an integer step. Sitting at the PHIS with  $\langle V \rangle = \frac{1}{2}$  and with  $i_{dc} \geq i_c^+$ , the size of the vortex pair increases and oscillates periodically in time, in phase with the ac current. This happens up to a time  $t_d$ , corresponding to a critical dipole size, after which the vortices break away from the pinning site. After  $t_d$  the moving vortices rapidly start generating other vortices, as shown in Fig. 3(a), which gives the total number of vortices,  $N_T = N_+ + N_-$ , defined by  $N_T = \sum_R |(1/2\pi) \sum_{P(R)} \phi_{ij}|$ , as a function of time. This vortex generation phenomenon does not appear to have been considered before. The motion of the vortices nucleated does not follow regular patterns, although in the one-defect case, and only in this case, they present a left-right antisymmetry, positive  $\leftrightarrow$  negative, about an axis along the current direction and passing through the defect, as shown in Fig. 3(b). The vortex nucleation continues up to another time  $t_{ACVS}$ , shown in Fig. 3(a). It is after this time that streets of vortices of alternating signs form with axial symmetry tilted by an average angle of about  $27^\circ$  measured clockwise with respect to the  $x$  axis, and separated along  $x$  by a distance of about  $L_x/2$ . The sign of the vorticity along each street oscillates in phase with the ac current. This ACVS is shown in Fig. 3(c). We have seen the ACVS also formed at an angle  $\pi - 27^\circ$ , as would be expected from symmetry considerations. This ACVS remains stable for the longest times we considered, which were several orders of magnitude larger than  $t_d$ . We found that the angle made by the ACVS is the same even when using free boundary conditions. In the latter case, however, the minimum lattice size needed to form the ACVS was  $64 \times 64$ . We studied

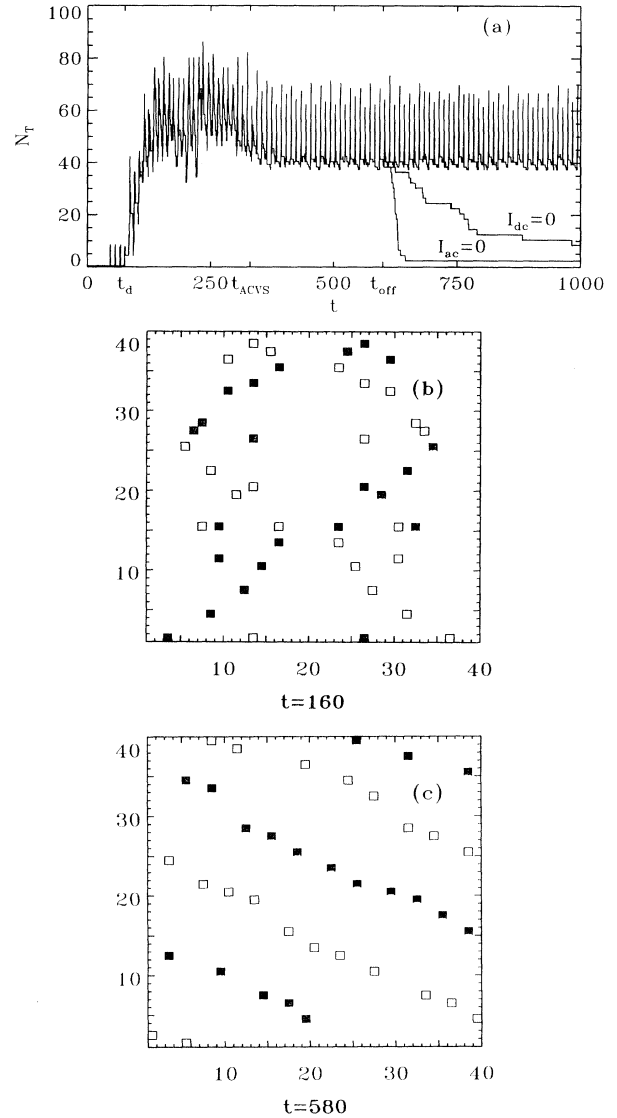


FIG. 3. Vortex dynamics for one defect with the same parameters as in Fig. 1(b). (a) Total number of vortices  $N_T$  vs time  $t$  for  $i_{dc} = 0.586$ . See text for definitions of  $t_d$ ,  $t_{ACVS}$ , and  $t_{off}$ . (b) Positive ( $\blacksquare$ ) and negative ( $\square$ ) vorticity ( $= \sum_{P(R)} \phi_{ij} = \pm 2\pi$ ) per plaquette at a time  $t_d < t < t_{ACVS}$ . (c) Same as (b) for the stationary ACVS configuration reached for  $t > t_{ACVS}$ .

the stability of the ACVS by varying  $i_{dc}$  or  $i_{ac}$  while in the  $\langle V \rangle = \frac{1}{2}$  plateau and did not see significant structural changes. The state does fall apart, though, when exiting the plateau. In Fig. 3(a) we see that for times larger than  $t_{ACVS}$ ,  $N_T$  has a minimum value of about  $L_y$ , while having large oscillations above this value at times corresponding to a period of twice that of the external ac current. We have also considered the cases when two, three, or all the lattice sites are disordered. The displacement of the sites is determined by choosing a random ra-

dus and angle distributed uniformly in  $[0, \epsilon]$  and  $[0, 2\pi]$ , respectively. We find that in all cases, although the length of the transient and the total number of ac-current-induced vortices is different, the stationary oscillatory state is essentially the same ACVS. This proves that this state is in fact very robust. To determine what is essential in the formation of the ACVS, we removed the defect at different delay times. When the defect is taken out at time  $t < t_d$ , the vortices do not have time to escape and they annihilate each other. However, when the defect is removed after time  $t \geq t_d$ , the two vortices are too far apart to annihilate each other and they are capable of generating the whole ACVS by themselves. This fact shows that *the defect is only a vehicle to generate the vortex pair but what is essential is to have at least two vortices sufficiently far apart to generate the ACVS*. To separate the relative importance of dc from ac currents in the stability of the ACVS, we turned off the ac current at a time  $t_{\text{off}}$  shown in Fig. 3(a). We see that the ACVS abruptly decays to the pinned two-vortex initial state. When the dc field was switched off, with the ac current still on, the ACVS stayed longer but eventually also decayed, as shown in Fig. 3(a). These results show that both the ac and dc currents are *essential* to generate and to maintain the stability of the ACVS. This is another of the basic differences with the GSS in which the oscillating vortex distribution remains after  $i_{\text{dc}}=0$ . To show that these results are not just a characteristic of the one-defect problem, in Fig. 1(c) we show the  $I$ - $V$  characteristic in the glass case, together with a blowup about the  $\langle V \rangle = \frac{1}{2}$  PHIS shown in Fig. 1(e). We note that there is a PHIS as well, and although the hysteretic effect is diminished, the pseudosteps are clearly present. Finally, we studied the stability of the ACVS against thermal fluctuations. In Fig. 2(b) we present results for the step width when increasing or decreasing the dc current as a function of the normalized temperature. Here we see that the ACVS is stable only at relatively low temperatures as compared to the phase-coherence critical temperature.

As can be gathered from the results discussed above, the ACVS we have discovered in our simulations is fundamentally different from the GSS. We suspect that the basic difference is that in order to explain the GSS one

uses a minimum-energy principle, while here the same does not appear applicable. An extensive discussion of these and other related results will be found elsewhere [9].

We thank R. Markiewicz and D. Stroud for very useful discussions and suggestions. The work presented here was partially supported by NSF Grant No. DMR-881-7933 and the Pittsburgh Supercomputing Center under Grant No. PHY88081P. We wish to thank the Donors of the Petroleum Research Fund, administered by the American Chemical Society, for the partial support of this research under Grant No. ACS-PRF#22036-AC6. Part of the work by D.D. was supported by a fellowship from CONICET, Argentina.

---

<sup>(a)</sup>Permanent address: Centro Atómico Bariloche, 8400 San Carlos de Bariloche, Rio Negro, Argentina.

- [1] For several papers on the subject see *Physica* (Amsterdam) **152B**, 1-302 (1988).
- [2] For a review see, C. D. Lobb, *Physica* (Amsterdam) **126B & C**, 319 (1989).
- [3] T. D. Clark, *Phys. Rev. B* **8**, 137 (1973); Ch. Leeman *et al.*, *Physica* (Amsterdam) **126B**, 475 (1984).
- [4] S. Benz *et al.*, *Phys. Rev. Lett.* **64**, 693 (1990).
- [5] K. H. Lee *et al.*, *Phys. Rev. Lett.* **64**, 962 (1990); J. U. Free *et al.*, *Phys. Rev. B* **41**, 7267 (1990); K. H. Lee and D. Stroud, *Phys. Rev. B* **43**, 5280 (1991); M. Octavio *et al.* (to be published).
- [6] H. Eikmans and J. E. van Himbergen (to be published); *Phys. Rev. B* **41**, 8927 (1990).
- [7] H. C. Lee *et al.*, *Physica* (Amsterdam) **165 & 166B**, 1571 (1990); *Phys. Rev. B* **44**, 921 (1991); S. H. Hebboul and J. Garland, *ibid.* **43**, 13703 (1991).
- [8] W. Xia and P. Leath, *Phys. Rev. Lett.* **63**, 1428 (1989); P. Leath and W. Xia, *Phys. Rev. B* (to be published).
- [9] D. Domínguez and J. V. José (to be published).
- [10] D. Gottlieb and S. Orzag, *Numerical Analysis of Spectral Methods: Theory and Applications* (Society for Industrial and Applied Mathematics, Philadelphia, PA, 1977).
- [11] H. S. Greenside and E. Hellfand, *Bell Syst. Tech. J.* **60**, 1927 (1981).